# A computational and experimental investigation of λ/2 and λ/4 sampling step in phaseless planar near-field measurements at 60GHz

**Álvarez, Javier Fernández; Breinbjerg, Olav**

*Published in:*
Proceedings of 12th European Conference on Antennas and Propagation

*Link to article, DOI:*
10.1049/cp.2018.0636

*Publication date:*
2018

*Document Version*
Peer reviewed version

# A Computational and Experimental Investigation of $\lambda/2$ and $\lambda/4$ Sampling Step in Phaseless Planar Near-Field Measurements at 60GHz

Javier Fernández Álvarez and Olav Breinbjerg
Department of Electrical Engineering, Technical University of Denmark, DTU
Kgs. Lyngby, Denmark
jafealv@elektro.dtu.dk, ob@elektro.dtu.dk

***Abstract*—While complex planar near-field measurements involve a formal sampling step requirement (less than $0.5\lambda$, typically $0.45\lambda$) phaseless planar near-field measurements with the two-scans technique do not. In phaseless measurements only the magnitude is measured; while the plane wave spectrum of the square of the magnitude has twice the bandwidth of the complex signal, the magnitude itself may have an even much larger bandwidth. However, the spectrum of the magnitude is not of significance for phaseless measurements with the two-scans technique where the measured magnitude is combined with an initial guess for the phase to form a complex signal. But this combined complex field may also have a plane wave spectrum that is broader than that of the measured complex signal and thus extend beyond the visible region of the spectral domain. This will happen if the initial guess for the phase does not fit properly to the measured magnitude; e.g. if the phase jumps by 180deg. at a point where the measured magnitude in non-zero. For this reason, the phaseless measurement may require a sampling step notably smaller than $\lambda/2$ to avoid aliasing effects in the visible region of the spectral domain. This work, based on experimental and simulated planar near-field measurements of a 60GHz horn, investigates the effect of the initial guess for the phase on the plane wave spectrum of the combined complex signal. Furthermore, it investigates the effect of the initial guess for the phase and different sampling steps on the phase retrieval, using the Iterative Fourier Technique, and thus on the resulting far-field radiation pattern.**

***Index Terms*—phaseless, magnitude-only, near-field, measurements.**

## I. Introduction

Phaseless near-field measurements are a diverse family of techniques which involve retrieving the phase of a given signal by means other than direct measurement; this is typically done by performing more measurements of the magnitude of said signal than is necessary for a complex measurement. They are desirable in situations when complex measurements are impractical or unreliable, such as measurements at high frequency when the fast-changing phase measure is more difficult to obtain due to inaccuracies of measurement equipment or probe positioning, cable bending, thermal drift, etc; while the magnitude of the measured signal is not significantly affected by these factors.

The two-scans phaseless technique [1]-[6] is based on a pair of magnitude measurements performed at two different distances from the antenna under test (AUT), and relies in the propagation relation between the fields at these two planes in order to retrieve a phase. This algorithm requires an initial guess for the phase, which may be any arbitrary phase with which one of the magnitude measurements is augmented. In complex near-field measurements the minimum sampling condition is met when a scan plane is sampled with a step size of half-wavelength. This ensures that evanescent plane waves become negligible, that the spectrum of the AUT is only non-zero in the visible region of the spectral domain, the circumference defined by $\sqrt{(}k_x^2 + k_y^2) < k_0$ (with $k_0 = 2\pi/\lambda$), and that the measurement is free of aliasing. However, the discrepancy between the initial phase guess and the real phase of the AUT results in a complex field that may no longer be contained within the visible region of the spectrum, as the phase may introduce spatial variations faster than $k_0$ or possibly discontinuities in the field. Therefore, while there is no formal requirement for denser than $\lambda/2$ sampling for this technique, it can be understood that the described situation is equivalent to an undersampled measurement.

In this paper a series of simulated and experimental results are presented, exploring the effects of the initial guess in the spatial bandwidth of the complex signal prior to phase retrieval. In addition to this, an investigation is presented on the impact of a denser $\lambda/4$ sampling in the accuracy of phase retrieval. By sampling more densely a better representation of the visible region and a larger alias-free region is obtained, and furthermore, thus resulting in a stronger convergence of the algorithm. In principle, it would be possible to investigate the effect of $\lambda/4$ vs. $\lambda/2$ sampling from entirely simulated data, however here we base the investigation on a set of measured near-fields on the first scan plane, in addition to a second set of simulated near-fields on the second scan plane, which are calculated from the first set of measured data.

This manuscript is structured as follows: in Section II a description of the AUT and measurement setup is given, in Section III the two-scans phaseless near-field technique is described, and the issue of sampling in phaseless measurements introduced, in Section IV the computational and experimental results are presented and discussed, and Section V contains the conclusions.

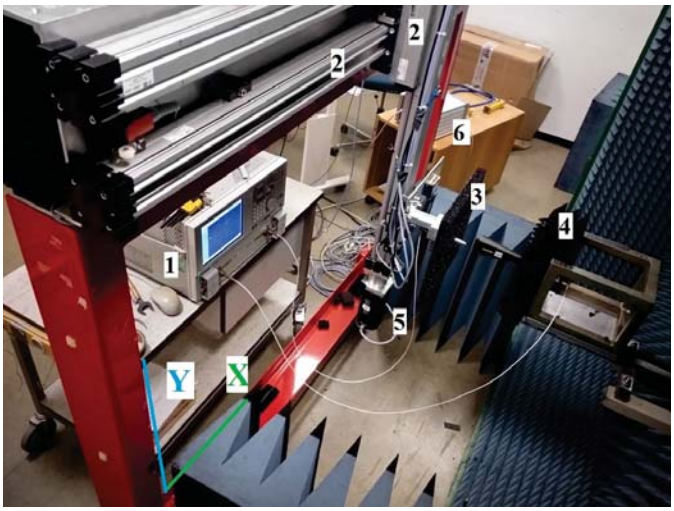


Fig. 1. DTU planar scanner setup showing Agilent VNA (1), linear actuators (2), open-ended waveguide probe (3), horn AUT (4) mounted in its frame, step motor (5) and motor controller (6). Homing position is shown as origin of the scanner coordinate system in bottom left of the image.

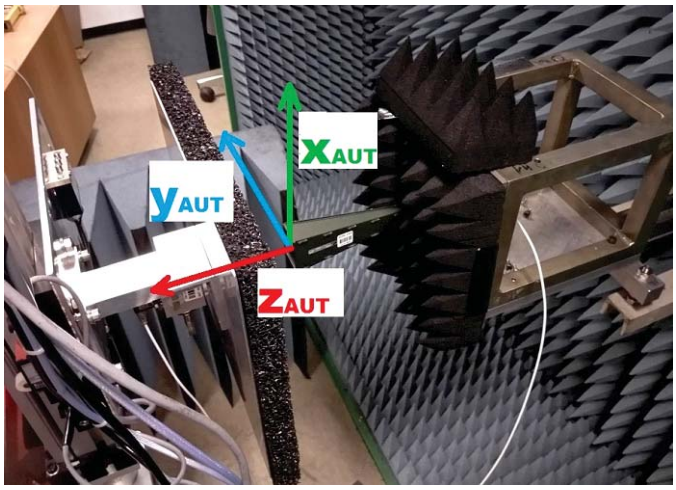


Fig. 2. Standard gain horn mounted in the AUT support frame with absorber material covering its front plate. The AUT coordinate system is also shown, with its center in the horn aperture.

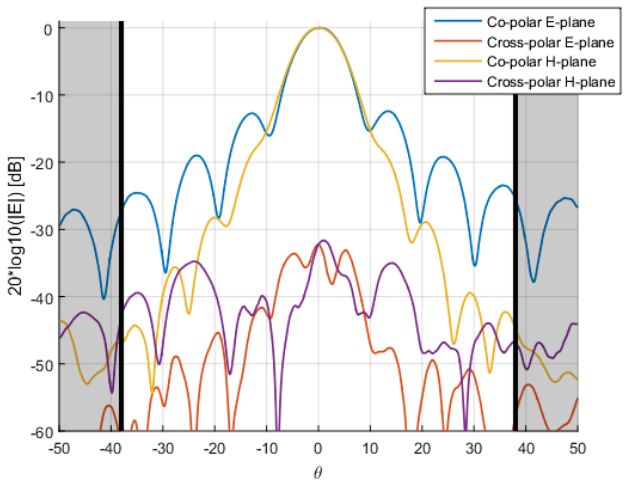


Fig. 3. Reference co- and cross-polar far-field patterns of the main cuts: E-plane ($\phi = 0$) and H-plane ($\phi = 90$).

## II. Antenna Under Test and measurement setup

The measurement setup in Fig. 1 is similar to the one described in [7] with only minor changes in length of the cables and disposition of absorbers in the non-anechoic room.

The AUT used in this work (Fig. 2) is a 25dBi Flann 24240-25 standard gain horn at a working frequency of 60GHz, with a rectangular aperture of 41mm by 30mm and a total length of 180mm. The aperture field is approximately modelled by a cosine-tapered magnitude and a phase with quadratic variation, and it is excited by a rectangular waveguide with a fundamental TE10 mode. The probe is a single-port, custom-made open-ended circular U-band waveguide with an aperture diameter of 4.9mm. The AUT x/y axes shown in Fig.2 are oriented parallel to the movement axes of the planar scanner (see in Fig.1), while the z axis is nominally parallel to the scan plane; in reality, the AUT sits on top of a metal rail which defines movement of the AUT in the longitudinal direction. The AUT is linearly polarized in the $y_{AUT}$ direction.

### A. Measured data

The area of the scanning planes is of 150mm x 150mm, identical to [7], where a phaseless measurement using half-wavelength sampling is reported, but the sample spacing has been now reduced to $\lambda/4 = 1.25$mm resulting in a matrix of 121 by 121 samples per scan plane. A scan was carried out at an AUT-probe distance of $z_1 = 30$mm ($6\lambda$), the two orthogonal components obtained by physically rotating the probe antenna by 90deg. Acquisition time was of 8h per component. The second set of data was calculated at $z_2 = 40$mm ($8\lambda$) by propagating the measured probe signals forward by means of plane wave expansion. The reference far-field patterns obtained from the $\lambda/4$ complex measurement at $z_1$ are shown in Fig. 3. The observed cross-polar component is a combination of mechanical misalignment of the setup and cross-polarization of the probe antenna, hence it does not present an on-axis dip, as is typical.

## III. Phaseless planar near-field technique

Phase retrieval by means of the Iterative Fourier Technique (IFT) [1] is based on a pair of near-field magnitudes measured at two different distances and an initial phase guess. This guess combines with one of the magnitudes to generate a complex field, hereby named *first complex near-field*, that is propagated from the first scan plane to the second scan plane. After this, the magnitude of said propagated field is discarded and substituted with the real, measured magnitude at the given scan plane. The complex field is then propagated back to the first scan plane, and the magnitude substituted again. Phase retrieval is performed independently on the two orthogonal components of the near-field because the $x$ and $y$ components

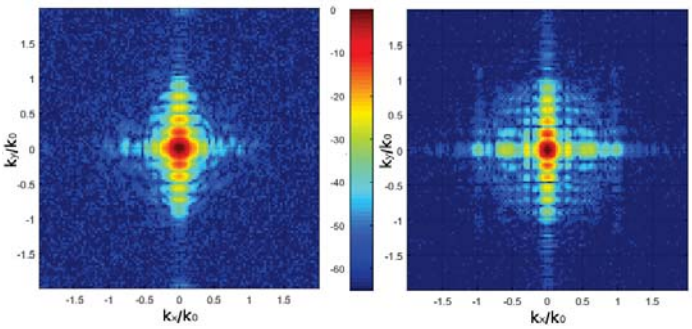


Fig. 4. PWS of measured AUT signal (left) vs PWS of first complex near-field described in Section IV, sampled at $\lambda/4$.

of the plane wave spectrum are completely decoupled. These operations of propagation and substitution are iterated until a certain condition is met, such as the minimization of an error metric. Optimally, this would mean that the initial guess has converged into the global minimum of the solution space, corresponding to the real phase of the signals measured at the scan planes. In practice this is not always true do perturbations of the magnitude measurements, such as measurement noise and finite dynamic range, which disturb the phase retrieval and cause it to become trapped in a local minimum of the solution. In particular, the IFT is highly sensitive to the initial guess, which to a great extent determines the optimal or erroneous convergence of the retrieved phase. Thus, it is critical that the initial guess does not introduce non-physical behaviours into the complex field [8] such as a phase null and sign reversal in a region where magnitude is non-zero which results in a discontinuity of the field. Nevertheless, the operation of augmenting the magnitude of the measured signal with an initial guess different than its real phase often results in spatial-domain variations faster than $k_0$, which give spectral components outside of the visible region. As is seen in Fig. 4, the plane wave spectrum (PWS) of the measured signal is different from the PWS of a first complex field created with the phase of a constant aperture as initial guess. The latter has a different shape, and overall larger level inside the visible region, but also has components outside the visible region that are not present in the PWS of the measured signal.

It can be understood that the amount of higher-order components introduced is related to how well the initial guess resembles the real phase: an guess such as an accurate model of the phase will typically result in a lower level of higher modes than a less precise model, or a simple guess such as a constant phase guess. Likewise, the iterative phase retrieval can be seen as a process of augmenting the measured magnitudes with a propagated phase that gradually converges to the real phase of the field, and therefore creates a spectrum gradually more confined to the visible region. To the best knowledge of the authors, there is no formal requirement for a sampling step smaller than $\lambda/2$ for phaseless measurements with the two-scans technique. However, for a field sampled at the minimum rate of $\lambda/2$, the plane wave spectrum (PWS) of the first complex

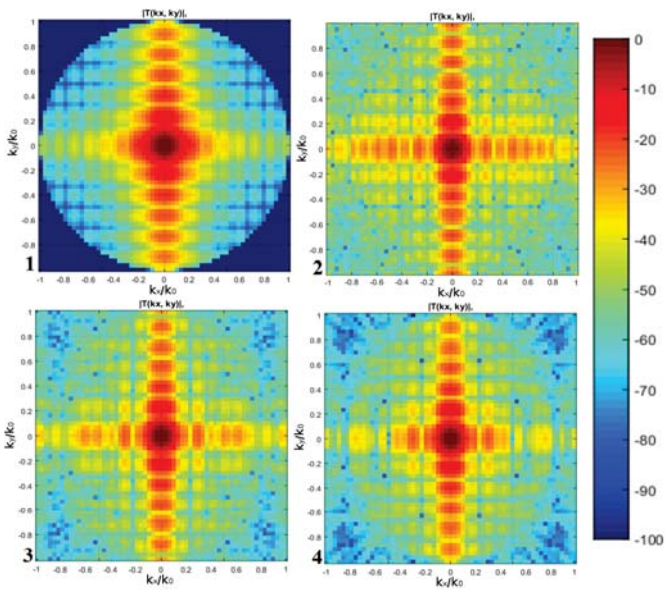


Fig. 5. PWS of simulated AUT NF (1) vs PWS of first complex near-field sampled at $\lambda/2$ (2), $\lambda/4$ (3) and $\lambda/10$ (4). Figures limited to $k_x, k_y < k_0$ domain.

near-field will be contaminated by the higher-order components of the periodic spectra aliasing in the visible region. Because of this, it is hypothesized that, for phaseless measurements by means of the IFT, a more precise result can be brought by denser sampling, allowing a closer representation of the visible region by reducing the aliasing of the discrete spectra.

## IV. Results and discussion

### A. Spectrum of first complex near-field

In light of Fig. 4, it is clear that the initial guess has an impact in the spatial bandwidth of the complex signal before phase retrieval. It then becomes apparent that denser than $\lambda/2$ sampling is desirable because it reduces higher-order components folding into the visible region. This can be demonstrated by comparing the visible region of the spectrum of the first complex near-field with different sampling densities. To this end, a model of the AUT is used, consisting of an aperture field with the dimensions of the AUT aperture, sampled with arbitrary step and propagated forward by means of plane wave expansion. With it, a near-field is simulated at a distance of 30mm from the aperture plane, its phase discarded and substituted with an initial guess. The guess is obtained from the same model, and it consists of the field from an identical aperture but with a constant magnitude/phase, instead of a quadratic distribution. This initial guess, though generic and involving minimal a-priori knowledge of the AUT, has been shown to provide good phase retrieval for this AUT [7], equivalent to more complex approximations of the real phase. Following this, for different sampling rates the PWS of the first complex near-field is calculated and compared.

As Fig. 5.1 shows, the real spectrum of the AUT near-field vanishes to zero outside the visible region. However, due to the discrepancy between the magnitude of the AUT field and the guessed phase, the first complex field varies in a different way than the real AUT field and this results in a level of ca. 50dB below maximum of components outside of the visible region, for a near-field sampled at $\lambda/2$ spacing (Fig 5.2). If the spacing is reduced to $\lambda/4$, or further down to $\lambda/10$ the level outside this region is visibly decreased by 5dB to 10dB (Figs 5.3, 5.4). Inside the visible region the effect is less evident as the initial guess raises the level also within this circumference (as corresponds to a more uniform phase than the real, which creates higher sidelobe level).

Substracting the $\lambda/2$ and $\lambda/4$ PWS, and normalizing to the maximum of the $\lambda/2$ PWS, leaves a difference of approximately -30 to -40dB in the $k_y$ axis (which corresponds to the E-plane) and between -40 to -60dB elsewhere in the visible region. If the $\lambda/2$ and $\lambda/10$ PWS are substracted the difference becomes larger. Since an increased sampling density changes the visible region it is clear that there must aliasing from the invisible region into the visible region for the coarse sampling and that this aliasing is reduced as sampling density is increased

### B. Influence of sampling rate in phase retrieval

The previous discussion on the influence of components outside of the visible region of the spectral domain is now applied to the task of phase retrieval. To this end, a comparison will be made between two phaseless measurements of the same AUT at two different sampling steps: $\lambda/4$ versus the standard $\lambda/2$. The objective of this comparison is to quantitatively evaluate the improvement of phaseless measurements by the reduction of spectral aliasing brought by denser sampling. The initial phase (Fig. 6) is the propagated phase of a uniform aperture field, the same as discussed in section IV.A. From each scan plane, a new set analogous to a $\lambda/2$ measurement of the AUT is created by extracting every second sample from the $\lambda/4$ measurement. This is done in order to eliminate potential sources of error due to repeatability (drift, cable bending, probe positioning, measurement noise), thus leading to a more meaningful comparison where the only factor that changes between the two phaseless measurements is the sampling density.

The retrieved near-field phases obtained as a result of the above are shown in Fig. 7. An inspection of the retrieved phases compared to the measured phase from Fig. 6 show that both retrieved phases are noisier than the measured signal: it is typically observed that the phase converges best in the areas of the scan plane where measured magnitude is stronger, and becomes noisier in samples with low field power. Comparing the two retrieved phases side by side points to a clear improvement in the $\lambda/4$ measurement. It is seen that the denser measurement results in a more defined, less noisy phase in the area of the horn aperture, and also clearer phase ridges along the $y$-axis. This improvement is directly confirmed in the radiation patterns shown in Figs. 7, 8, where the $\lambda/4$ clearly shows a better agreement to the complex measurement. The accuracy

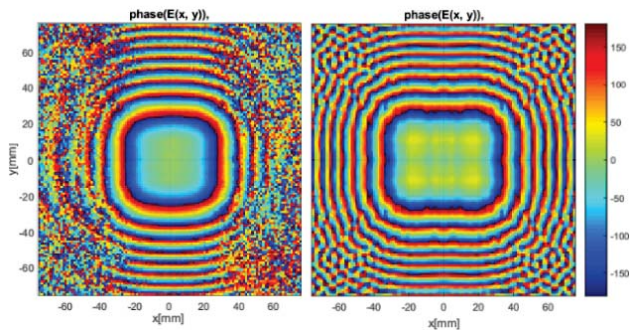


Fig. 6. Near-field co-polar measured phase at $z_1 = 30$mm (left) vs phase of first complex near-field (right).

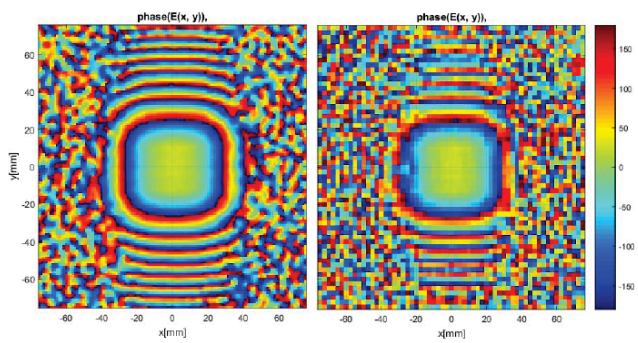


Fig. 7. NF co-polar retrieved phase at $z_1 = 30$mm with $\lambda/4$ sampling (left) vs $\lambda/2$ sampling (right).

of the retrieved far-field patterns is quantitatively assessed by means of the Equivalent Error Signal (EES) calculated between the phaseless measurement and the complex reference pattern. It is then seen that for the $\lambda/2$ case the EES of the co-polar component remains at a level of -40dB within the region of validity, whereas the EES in the $\lambda/4$ co-polar pattern is consistently smaller by as much as to 10dB within this region.

Since sampling density is the only variable in this experiment, the previous results point to the hypothesis in section III that measuring the magnitude of a field with a sampling step smaller than the general $\lambda/2$ spacing is beneficial for phaseless measurements as it reduces aliasing on the PWS of the signal propagating between scan planes.

### C. Mechanical alignment accuracy

An interesting aspect of phaseless measurements revealed during the scope of this work is a dependency of the phase retrieval algorithm with the correct alignment of the AUT at the two scan planes. Post-processing of the measured data, which included an additional measurement at the second $z_2$ scan plane, showed a small displacement of the near-field magnitudes, as the points of maximum measured magnitude at $z_1$ and $z_2$ were shifted in the scanner coordinate system. This results in a serious problem for the two-scans technique: from the point of view of the IFT, this situation is analogous to an AUT with a squinted main beam and thus the retrieved phase converges to accommodate for this squinting, resulting in

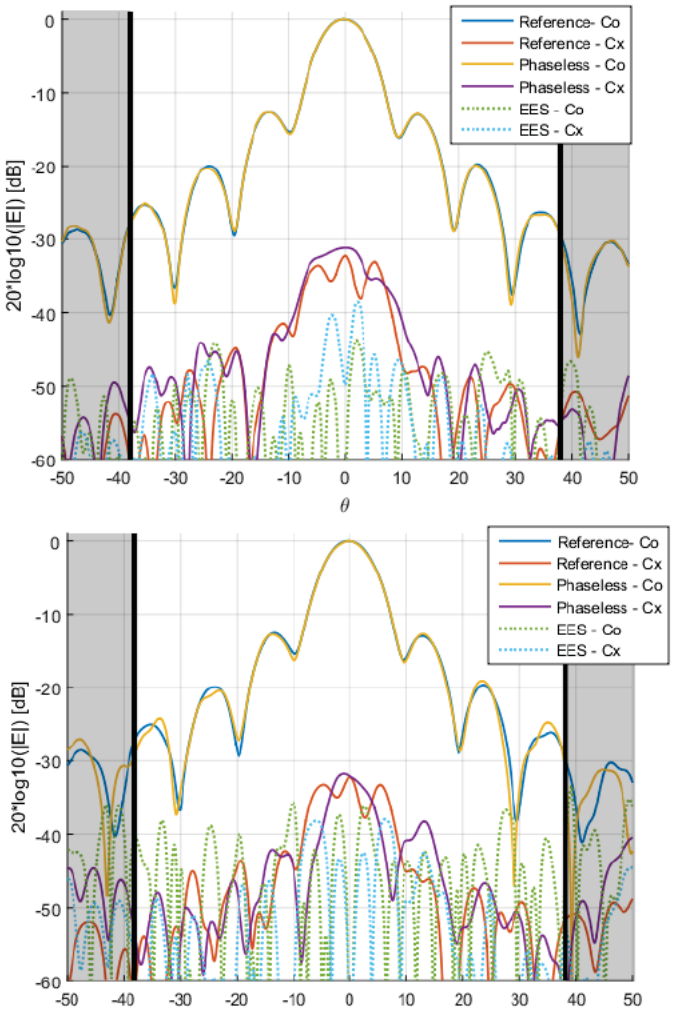


Fig. 8. Retrieved FF E-plane ($\phi = 90$) patterns using $\lambda/4$ measurement data versus $\lambda/2$ data. Co- and cross-polar components shown. The retrieved FF patters are respectively compared to the complex reference pattern by means of EES. The angular region of reliability is marked by the vertical black lines.

an erroneous phase retrieval. The cause for this translation of the data was most likely a displacement of the AUT frame on the z-axis rail. Interestingly, this accidental translation, which is estimated at 0.8mm from the squinting of the main beam, was previously masked by the coarse $\lambda/2$ sampling and thus gave no beam squint, but it was detectable by the finer $\lambda/4$ sampling and thus gave rise to beam squint.

Therefore, in addition to the benefits brought by $\lambda/4$ sampling to phaseless measurements, there is also a stricter requirement on probe-AUT alignment needed in order to overcome this issue; this is because at this high frequency, and with such a small sampling step even a small displacement of the AUT can create a noticeable squint in the far-field pattern.

## V. Conclusions

While there is no formal requirement for a sampling step smaller than half a wavelength for phaseless measurements with the two-scans technique, it has been demonstrated here that a sampling step of quarter a wavelength gives a far-field radiation pattern in clearly better agreement with the reference pattern obtained from a complex measurement. It has been shown that this is due to the fact that the combination of the measured magnitude and an initial guess for the phase can result in a complex field with a spectral bandwidth larger than the visible region, and with only half a wavelength sampling this spectrum is undersampled and thus aliasing occurs in the visible region.

In principle, the combination of the measured magnitude and the initial guess for the phase could possess an even broader spectral bandwidth than what can be recovered with a quarter wavelength sampling. However, in practice the quarter wavelength sampling is already challenging since it requires four times the number of measurement samples of a half wavelength sampling.

It has been demonstrated that the phaseless two-scans technique is very sensitive to small translations of the antenna under test parallel to the scan plane(s) between the two measurements, which the phase retrieval "sees" as a squinting of the radiation pattern, and thus converges to a complex near-field with linear phase variation and thus a far-field beam squint.

## Acknowledgment

This work was supported by the European Space Agency through ESA contract no. 4000113496/15/NL/Mh/ats "Phaseless Near Field Antenna Measurements". The authors thank Maurice Paquay, ESTEC, for his input to this work.

## References

[1] A. P. Anderson, and S. Sali, "New possibilities for phaseless microwave diagnostics", *IEEE Proceedings H (Microwaves, Antennas and Propagation*, vol. 132, no. 5, pp.291-298, 1985.

[2] T. Isernia, G. Leone, and R. Pierri, "Phaseless Near Field Techniques: Fomulation of the Problem and Field Properties", *Journal of Electromagntic Waves and Applications*, vol. 8, no. 7, pp. 871-888, 1994 and "Phaseless Near Field Techniques: Uniqueness Conditions and Attainment of the Solution", *Journal of Electromagntic Waves and Applications*, vol. 8, no. 7, pp. 889-908, 1994.

[3] S.F. Razavi and Y. Rahmat-Samii, "A New Look at Phaseless Planar Near-Field Measurements: Limitations, Simulations, Measurements, and a Hybrid Solution", *IEEE Antennas and Propagation Magazine*, vol. 49, no. 2, pp. 170-178, April 2007.

[4] T. Isernia, G. Leone, and R. Pierri, "Radiation Pattern Evaluation from Near-Field Intensities on Planes", *IEEE Transactions on Antennas and Propagation*, vol. 44, no. 5, pp. 701-710, 1996.

[5] R.G. Yaccarino and Y. Rahmat-Samii, "Phaseless bi-polar planar near-field measurements and diagnostics of array antennas", *IEEE Transactions on Antennas and Propagation*, vol. 47, no. 3, pp. 574-583, March 1999.

[6] S.F. Razavi and Y. Rahmat-Samii, "Polarization Extraction in Planar Near-Field Phaseless Measurements", *IEEE Transactions on Antennas and Propagation*, vol. 56, no. 10, pp 3233-3240, October 2008.

[7] J. Fernandez Alvarez, S. Pivnenko, and O. Breinbjerg. "Probe-Corrected Phaseless Planar Near-Field Antenna Measurements at 60 GHz", *Proceedings of the 37th Annual Symposium of the Antenna Measurement Techniques Association*, Long Beach, CA, USA, pp 314–319, 2015.

[8] O. Breinbjerg and J. Fernandez Alvarez. "Phaseless Near-Field Antenna Measurement Techniques – An Overview", *Proceedings of the 38th Annual Symposium of the Antenna Measurement Techniques Association*, Austin, TX, USA, pp 314–319, 2016.